



SqueezeMe: Creating Soft Inductive Pressure Sensors with Ferromagnetic Elastomers

Thomas Preindl*

Faculty of Engineering

Free University of Bozen-Bolzano

Bozen-Bolzano, Italy

tpreindl@unibz.it

Andreas Pointner*

Faculty of Engineering

Free University of Bozen-Bolzano

Bozen-Bolzano, Italy

apointner@acm.org

Nimal Jagadeesh Kumar

School of Engineering and

Informatics

University of Sussex

Brighton, United Kingdom

nimaljkumar2@gmail.com

Nitzan Cohen

Faculty of Design and Art

Free University of Bozen-Bolzano

Bolzano, Italy

nitzan.cohen@unibz.it

Niko Münzenrieder

Faculty of Engineering

Free University of Bozen Bolzano

Bozen-Bolzano, Italy

niko.muenzenrieder@unibz.it

Michael Haller

Faculty of Engineering

Free University of Bozen-Bolzano

Bolzano, Italy

michael.haller@unibz.it

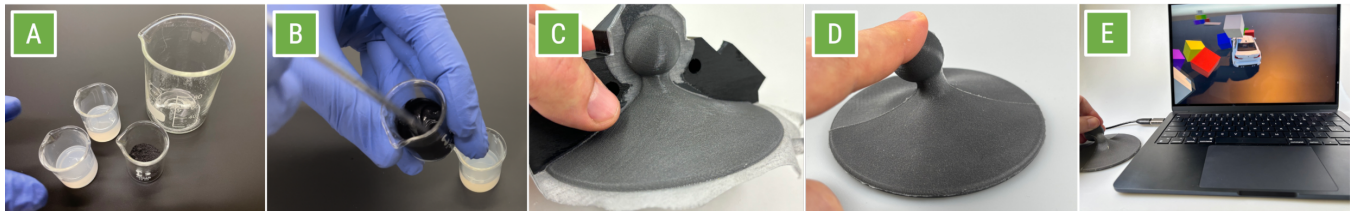


Figure 1: In SqueezeMe, ferromagnetic particles are mixed with elastomers (A, B), allowing us to cast more complex 3D sensors (C), which ultimately serve as joysticks (D) for various applications (E).

Abstract

We introduce SqueezeMe, a soft and flexible inductive pressure sensor with high sensitivity made from ferromagnetic elastomers for wearable and embedded applications. Constructed with silicone polymers and ferromagnetic particles, this biocompatible sensor responds to pressure and deformation by varying inductance through ferromagnetic particle density changes, enabling precise measurements. We detail the fabrication process and demonstrate how silicones with varying Shore hardness and different ferromagnetic fillers affect the sensor's sensitivity. Applications like weight, air pressure, and pulse measurements showcase the sensor's versatility for integration into soft robotics and flexible electronics.

CCS Concepts

- Hardware → Sensor applications and deployments; • Computer systems organization → Sensors and actuators.

*Authors contributed equally to this research.



This work is licensed under a Creative Commons Attribution 4.0 International License.
CHI '25, Yokohama, Japan

© 2025 Copyright held by the owner/author(s).
ACM ISBN 979-8-4007-1394-1/25/04
<https://doi.org/10.1145/3706598.3713369>

Keywords

Fabrication, Sensors, Tangible, Artifact or System, Prototyping/Implementation

ACM Reference Format:

Thomas Preindl, Andreas Pointner, Nimal Jagadeesh Kumar, Nitzan Cohen, Niko Münzenrieder, and Michael Haller. 2025. SqueezeMe: Creating Soft Inductive Pressure Sensors with Ferromagnetic Elastomers. In *CHI Conference on Human Factors in Computing Systems (CHI '25), April 26–May 01, 2025, Yokohama, Japan*. ACM, New York, NY, USA, 13 pages. <https://doi.org/10.1145/3706598.3713369>

1 Introduction

Functionalized soft materials offer new possibilities for human-computer interaction, enabling more intuitive and flexible interfaces compared to rigid interfaces. Traditional systems rely on explicit interactions, such as binary state buttons or voice commands, which, while efficient, often lack the adaptability and seamless integration needed for more natural, embodied interactions. In contrast, soft tactile interfaces can support implicit, gradual input and mimic the mechanical properties of natural objects and the human body [6, 9, 14, 28]. In contrast to Ozioko's work [23], in this paper we aim to contribute to the field of deformable interfaces by demonstrating how highly sensitive soft sensors, shaped in a wide range of geometries, can be implemented using various silicones and filler materials, in a simple manufacturing process.

SqueezeMe presents, a highly flexible inductive pressure sensor made from ferromagnetic elastomers and an appendant coil,

designed for precise pressure sensing in wearable and embedded applications. The elastomer is constructed using silicone polymers mixed with ferromagnetic particles, creating a soft and flexible material which permeability responds to deformation and applied pressure. The sensor coils inductance changes with deformation of the attached elastomer due to variations in the density of the ferromagnetic particles within the elastomer matrix, enabling high-precision measurements. Unlike many related works, our approach is very simple to implement and requires minimal technical effort. Moreover, the implementation using a inductive coil is straightforward and allows precise detection of small, subtle interactions through pressure or deformation - even with complex shapes.

We detail the fabrication process and demonstrate how different silicones, with varying Shore hardness levels and ferromagnetic fillers, respond to pressure. Additionally, we showcase various applications, demonstrating the sensors sensitivity with various weights, through a game controller, a squeezable fidget toy, an air pressure sensor, and a pulse monitoring device, illustrating the versatility and potential of the sensing principle.

In summary, the contributions of this work are as follows:

- **Development of *SqueezeMe*:** A highly flexible and soft arbitrarily shapeable inductive pressure sensor constructed from (biocompatible) ferromagnetic elastomers, designed for precise pressure sensing across diverse applications.
- **Detailed fabrication process:** A comprehensive guide to constructing soft sensors using different silicone polymers with varying Shore hardness and ferromagnetic fillers.
- **Material analysis and sensor response:** A systematic investigation of various filler material and silicone combinations, providing insights into the relationship of softness, filler material and sensor precision.
- **Design flexibility for diverse applications:** Demonstration of the sensor's versatility in scenarios such as weight measurement, pulse monitoring, and integration into game controllers.

2 Related Work

Stretchable and deformable interfaces are garnering increased interest in the development of next-generation technologies due to their potential to create more natural and intuitive user experiences. This is shown among many other examples through the development of shape displays [10], foldable interactive objects [22], and yarn-based pressure sensing [26].

2.1 Deformable User Interfaces

Deformable User Interfaces (DUIs) offer novel interaction methods through physical manipulation of flexible devices. These interfaces allow for intuitive, dynamic control, yet many prior works lack focus on high-sensitivity pressure sensing for wearables and tangible interactions. *SqueezeMe* builds upon these advances by prioritizing sensitivity and shape flexibility. For instance, the *Skin-On* project added artificial skins to devices like smartphones, allowing intuitive gestures such as pinching and twisting, enhancing tactile interaction by mimicking the human skin [32]. Similarly, *Stretchis* uses stretchable materials to manipulate digital content, supporting gestures like pulling and pinching for a tactile, immersive experience

[36]. The project integrates sensors and displays onto PDMS substrates, creating customizable interactive surfaces. *SOFTii* offers continuous control via pressure-based input [21], while *HandLog* uses conductive foam sensors to map hand gestures for real-time input, particularly in gaming and rehabilitation [4]. Follmer et al. used Ecoflex and Dragon Skin 10 in jamming interfaces to achieve flexibility and transparency in various shapes [9]. *iSkin* introduces a flexible, stretchable sensor technology for interactive skin-worn interfaces. It utilizes a silicone-based material embedded with capacitive sensors to enable touch, swipe, and pressure inputs directly on the skin. [35] Similarly, other works have used Ecoflex for flexible membranes and strain sensors [1, 29]. One example is *Flexibles*, introduced by Schmitz et al. [27], where flexible tangibles can capacitively detect various user interactions, including pressing, squeezing, and bending. Fabricated in a single pass using consumer-level 3D printers, *Flexibles* require no additional assembly and can be customized in geometry and functionality. This approach was also an inspiration for our work, as the main goal was to come up with a concept that also allows developers to design more complex geometries.

These works contribute foundational methods for deformability in interfaces but often lack detailed pressure sensitivity analysis or application adaptability, which *SqueezeMe* addresses through its highly responsive ferromagnetic elastomer sensors with inductive readouts.

We drew inspiration from the projects, *Squeezaplus* and *Squishy, Yet Satisfying*. *Squeezaplus* inspired us in translating squeezing actions into digital commands. In *Squishy, Yet Satisfying*, the authors investigated how people associate deformable shapes with colors and emotions. These studies informed our sensor's application versatility and sensory feedback potential, highlighting opportunities for enhancing user interaction experiences through material feedback in flexible form factors. [30]

2.2 Manufacturing a Deformable User Interface

Similar to our approach, many researchers developed squeezable interfaces using the soft polymer Polydimethylsiloxane (PDMS). For example, Ngyuen et al. used PDMS, an Indium Tin Oxide (ITO) coated PET films, and conductive foam in layers to create a flexible, deformable surface capable of detecting pressure and bending [21]. This multilayer configuration is effective for basic deformation sensing but does not achieve the precision of inductive pressure sensing techniques enabled by our ferromagnetic elastomers. On the other hand, the *Squeezaplus* authors utilized silicone rubber compounds to create soft cavities through silicone casting methods, often with 3D-printed molds [14].

Our work was mainly inspired by the studies of Kumar et al. [19] and Ozioko et al. [24], which explore ferromagnetic elastomers in varied applications. While these works primarily focused on combining Ecoflex with ferromagnetic materials, we took it a step further by combining different types of silicone with various particles. Additionally, our paper presents diverse applications, demonstrating that the concept works beyond simple geometries. Finally, we provide detailed information, enabling also novices to replicate this approach relatively easily.

Building on these foundations, we adapt the implementation methods and provide detailed insights into designing a stretchable silicone-based sensor. Building on Kumar's et al. applications we extended the possible applications of the sensor design and furthermore explored the design decisions in the fabrication. Bira et al. offer an extensive overview of magnetic elastomers. Their review covers the various types of magnetic elastomers, their material properties, and their applications, such as in actuators and damping systems [5]. SqueezeMe advances these insights by integrating ferromagnetic elastomers with the user-friendly fabrication of deformable, interactive devices, emphasizing real-time applications that these reviews only indirectly address.

2.3 Inductive Sensing in HCI

Inductive sensing has been widely explored in HCI research, as demonstrated in works such as [7, 11, 13]. While existing works, such as *Indutivo*, focus on sensing conductive objects, they do not fully explore the sensitivity and versatility required for wearable pressure sensors, which we aim to address. For example, in the paper *Indutivo*, the authors introduce a contact-based inductive sensing technique designed to interact with conductive objects. This system detects and tracks everyday conductive items, recognizing motions like sliding, hinging, and rotating by leveraging changes in electromagnetic fields to identify object characteristics and movements [13]. In a subsequent paper, the authors presented *Tessutivo*, an inductive sensing method enabling contextual interactions on interactive fabrics [12].

More recently, Mao et al. developed a highly elastic inductive sensor made from liquid metal, capable of detecting a wide range of strains with excellent durability. While this sensor is highly flexible, SqueezeMe offers an alternative approach using ferromagnetic elastomers, enhancing the material's stability and form adaptability for interactive use cases beyond wearable health monitoring. This sensor is used in wireless setups to monitor human activities like breathing, swallowing, and joint movements, proving effective health monitoring and wearable applications [20]. One related work by Ozioko et al. presented an inductance-based pressure sensor using various compositions of iron particles in *Ecoflex* to improve sensitivity and recovery time [24]. In contrast to their paper, we focused on creating versatile, shapeable sensors with applications spanning joysticks, pulse monitors, and wearable devices. While their work investigates the effect of varying iron-to-Ecoflex ratios on sensor performance for robotics and tactile sensing, we explored diverse fabrication techniques, using both Ecoflex and Mold Star with varying hardness, different filler materials and filler particle sizes. Further, our approach highlights adaptability for multiple form factors and broader applications, including lightweight measurements and interactive devices. Summarizing, SqueezeMe's unique material composition allows for a more customizable and responsive sensor than prior approaches.

3 Design and Manufacturing

In this paper, we utilize inductors that are sensitive to the presence and properties of a surrounding ferromagnetic composite. This composite is composed of ferromagnetic *microparticles* ($30\text{ }\mu\text{m}$ – $150\text{ }\mu\text{m}$) embedded in a soft elastomeric structure, which serves as the coil's

core. The ferromagnetic particles are chosen for their high magnetic permeability. The overall permeability of the soft core is determined by the low permeability of the elastomer, the high permeability of the ferromagnetic filler, and the density of the ferromagnetic particles within the elastomer matrix. The coil's inductance is influenced by its geometry, core size, and effective permeability. Greater permeability and larger core sizes enhance the inductance, reducing the impact of parasitic resistances. When mechanical stress is applied, compressing or stretching the material, the density of the ferromagnetic particles changes, altering the core's effective permeability and size. This directly affects the inductance of the coil, which can be measured electrically.

3.1 Casting Ferromagnetic Elastomers

Soft devices with mechanical or electrical functionality can be realized in many ways, including solution-based processes, printing, thin-film technology, various transfer methods, textile manufacturing methods, or the creation of functionalized composites [8]. When it comes to materials that are flexible, stretchable, soft, arbitrarily shapeable, and compatible with these fabrication technologies, silicones are the preferred choice in both research and industry. Silicones are polymers made from siloxane, which contain silicon and organic groups, and are used in products such as oils, rubbers, and resins. In particular, rubbers made from silicone offer the mechanical and chemical properties, as well as stability required for the realization of biocompatible soft devices. They can be cured into virtually any shape and are available in a variety of formulations.

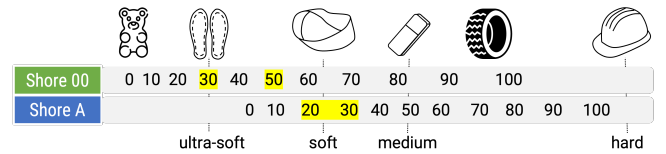


Figure 2: We used elastomers with different hardness levels, specified in Shore 00 and Shore A. Ecoflex, with Shore 00-30 and 00-50, was the softest amongst our specimens, while Mold Star was a bit less soft with Shore A-20 and A-30. Note that the alignment of the two hardness scales can only be an approximation, as the different scales use different methods of measuring hardness.

The silicone *Ecoflex* is biocompatible, making it ideal for wearables and implants, leading to its widespread use in stretchable on-skin electronics [19]. When we refer to biocompatibility, we specifically address both tissue and immunologic biocompatibility, as defined by Park et al. [25], who confirmed the biocompatibility of Ecoflex in the context of implantable flexible electronics. Since the ferromagnetic particles must not come into direct contact with the sensing coil, they can be safely embedded within pure Ecoflex, ensuring the biocompatibility of the sensor system. When fissures in the silicone are a concern, magnetite particles can be coated in a way so that they are biocompatible, as shown by [31] and [33]. The silicone *Mold Star* is a more affordable elastomer, often used for casting silicone molds, with a curing time of under an hour. Besides their use as substrate, silicone rubbers can be mixed also

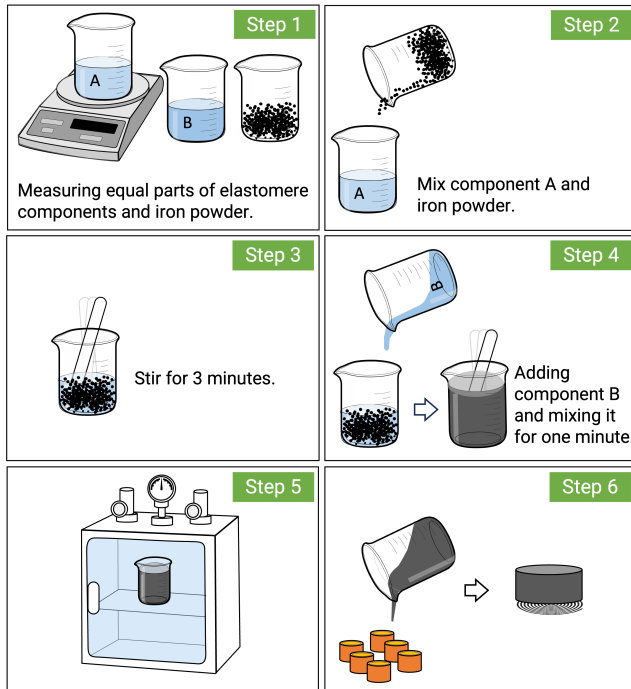


Figure 3: To implement a ferromagnetic silicone, six steps were necessary (1-6).

with functional fillers during the curing process. These are often conductive to realize soft electrodes or piezoresistive composites for sensor applications [18]. Similarly, ferromagnetic fillers, like iron, nickel, cobalt or their oxides ($\mu_r > 1000$), combined with elastomers are of interest in magnetic connectors on wearables[17] as they can lead to soft composites with high magnetic permeability [19].

Elastomers are available as two-component products: component (A), the silicone, and component (B), usually the curing agent. The material itself is primarily characterized by its hardness, which is measured using the Shore scale, cf. Figure 2. The hardness on a Shore scale is a dimensionless measure determined by measuring the percentual indentation depth using a specific indenter and force. The hardness of the two silicones we use are specified using two different Shore scales (Shore 00 for EcoFlex and Shore A for Mold Star) which cover different hardness ranges, as shown in Figure 2. The scales can not be directly converted from one to the other, as they use different measurement parameters, but can be compared using the provided hardness comparison shown in Figure 2.

In our work, we mainly used two materials: Ecoflex and Mold Star. It is important to note that Ecoflex specifies hardness using the Shore 00 scale, while Mold Star uses the Shore A scale. We will discuss this in more detail in the experiments later on, but generally, we conducted tests with Shore 00-30 and 00-50 (using Ecoflex) and Shore A-20 and A-30 (using Mold Star) to cover a hardness range from ultra-soft to soft.

Figure 3 provides an overview of the manufacturing process for ferromagnetic silicone. Equal parts of component A and component B of the elastomer, and the ferromagnetic particles in an 1:1:1 ratio

were prepared (Step 1). After preparing the appropriate amounts, the metal particles (Step 2) were carefully mixed with the silicone (typically component A) under a fume hood and stirred thoroughly for about three minutes (Step 3). Following this, the hardener (usually component B) was added and stirred into the mixture for one minute (Step 4). The mixture was then promptly placed in a vacuum chamber to remove air bubbles (Step 5). Under vacuum, the trapped air caused the mixture to expand. It was left in the chamber until it collapsed again, indicating that most air bubbles had been removed. Once this point was reached, the vacuum pump was turned off, the chamber was returned to room air pressure and the mixture was quickly poured into a mold (Step 6).



Figure 4: Different molds were FDM printed for our experiments. For example, three different shapes were used to create a 3D controller (A). For a squeezer, we developed a concave geometry (B). For a tire, three components were printed to ensure that the cast form could be easily removed (C).

We primarily used 3D printed molds (cf. Figure 4) using Polylactic acid (PLA) filaments. The used silicone cured without problems in the PLA molds. When using different silicones it is important to test the compatibility of the silicone and the mold material. It is advisable to design the negative molds in a way that allows them to be disassembled, making it easier to remove the silicone samples. Additionally, it is beneficial to spray the mold with a release agent, so that the silicone can be removed more easily. It is important to note that the negative mold should never be made of silicone itself, as even if the negative mold has fully cured, the silicone samples can bond with it, destroying the mold.

3.2 Sensor Coils

To measure the inductance, we need to use a suitable coil. In our experiments, we tested and implemented various options, including placing a planar PCB coil beneath the magnetic elastomer mold (see Figure 5).

Additionally, we wrapped an insulated wire (e.g., Electrisola TW-A, 0.16 mm) around the mold, and finally we also tested a variation where the insulated wire was wound and then embedded into the mold. Every approach has its advantages and drawbacks which we will discuss in the following sections.

4 Inductive Sensing

Inductive sensors work by generating a magnetic field around a conductor and detecting changes in inductance caused by the presence or movement of a conductive or ferromagnetic object within the field. The ferromagnetic material (with high magnetic permeability) alters the distribution of the magnetic field around the coil. This change directly impacts the coil's inductance, which is its ability to store energy in the magnetic field.

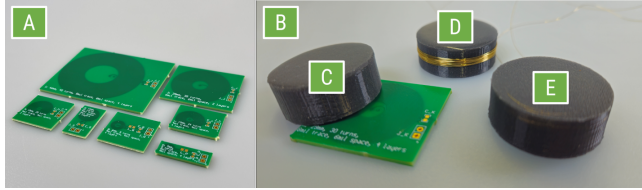


Figure 5: Three different approaches to integrating ferromagnetic silicone are proposed (B). The first method involves simply placing it on a planar PCB coil (A) positioned beneath the silicone (C). The second method involves securing the coil around the silicone (D). Lastly, the third approach involves embedding the coil within the silicone itself (E).

The soft inductive pressure sensor described in this paper consists of a coil, a soft ferromagnetic core, and a capacitor. The sensor's inductance is influenced by the geometry and material properties of both the coil and the core, as well as the surrounding environment. When the silicone core, embedded with ferromagnetic particles, is compressed, its permeability and shape change, which influences the inductance.

The permeability of the material within the elastomer is the most critical property of the sensor, as it directly affects the coil's inductance. Higher permeability materials result in a higher inductance.

The measured inductance is influenced not only by the deformation of the silicone cylinder but also by its placement. The proximity of a person's body or limbs can affect the measured inductance, though to a lesser extent than the deformation of the silicone cylinder itself.

In our experiments, the coil is either a flat spiral on a printed circuit board or a helical hand-wound coil made from enameled wire. For the flat coil, the core material is placed on top, cf. Figure 5 (C). For the helical coils, they are either embedded within cast silicone (cf. Figure 5, E) or wound around a cured silicone core, cf. Figure 5 (D).

The inductance of the coil is determined by measuring the frequency of a resonant LC circuit consisting of the coil (L) and a parallel capacitor (C). The resonant frequency of the LC circuit depends on the coil's inductance, the chosen sensor capacitor, and the parasitic capacitance of the circuit. The inductance L is then calculated as:

$$L = \frac{1}{(2\pi f_{\text{SENSOR}})^2 C} \quad (1)$$

where f_{SENSOR} is the measured resonance frequency, and $C = C_{\text{SENSOR}} + C_{\text{PARASITIC}}$.

For all experiments and demonstration applications, we used the LDC1614 inductance-to-digital converter from Texas Instruments, controlled by the MSP430 microcontroller. The LDC1614 was selected for its 4-channel capacity, 28-bit resolution, and wide sensing frequency range from 1 kHz to 10 MHz.

The LDC1614 outputs a frequency, f_{SENSOR} , in Hertz, which is then converted to an inductance, L , in Henry, based on the sensing capacitance, C . In our experiments, we used capacitors ranging from $1 \mu\text{F}$ to 1nF , depending on the inductance of the sensing coil. The data provided by the MSP430 microcontroller was streamed via USB to a host computer using a Python script, which transmitted

the data to other software via OSC and/or the ZMQ protocol. For visualization, the inductance values were displayed using the VVVV visual programming platform and Unity.

Inductors (i.e., coils) possess inherent parasitic capacitance, which varies depending on their construction and geometry. At the Self-Resonant Frequency (SRF), the reactance of the inductor cancels out the reactance of the capacitance. Due to the instability and difficulty in controlling parasitic capacitance, the LDC1614 datasheet recommends keeping the sensor frequency below 0.8 times the SRF for stable operation. This informs the choice of the sensor capacitor, and thereby the sensor frequency.

5 Experiment: Evaluating ferromagnetic particles, silicones and sensing coils

To investigate the properties of silicone materials when combined with various ferromagnetic fillers, we conducted a study. This experiment utilized two silicone rubber products, Ecoflex and Mold Star, commonly employed in research for molding, modeling, and creating flexible prototypes. These materials were selected for their distinct mechanical properties, which make them suitable for a wide range of research and development applications. Mold Star is known for its durability and high tear resistance, making it ideal for reusable molds. In contrast, Ecoflex is softer, highly flexible, and recognized for its biocompatibility and extreme compliance, capable of stretching up to 900% [15, 34]. In this study, we used Ecoflex 00-30 with a Shore hardness of 00-30 and Mold Star 31T (31T being the product descriptor) with a Shore hardness of A-30. Ecoflex can be stretched significantly without tearing. While it does not have the same tear resistance as Mold Star, its ability to flex and bend repeatedly without losing its shape makes it ideal for applications requiring continuous movement or wearability [19].

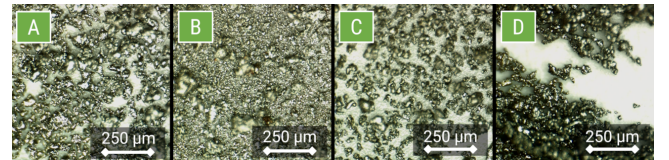


Figure 6: Overview of the various iron powders used in the second experiment as seen under a microscope with 40x magnification: Ancorsteel 1000C Powder (A), Fine Iron Powder (B), Coarse Iron Powder (C), and Magnetite Powder (D).

For the experiment, we combined both elastomers with four different fine iron powder fillers, including Ancorsteel 1000C Powder (150 μm), Iron Powder Fine (30 μm), Iron Powder Coarse (90 μm), and Magnetite Powder (63 μm), cf. Figure 6. All of these metal particles are ferromagnetic and exhibit a high permeability. We chose Ancorsteel 1000C primarily because it is more widely used (in 3D printing) and has a relatively large particle size. In contrast, we also selected a very fine iron powder, a medium iron powder, and finally, magnetite powder as recommended by Kumar et al. [19].

Working with Mold Star 31T has to be done more quickly, as it needs to be processed within three minutes once the components are mixed, and hardens much faster compared to Ecoflex. On the other hand, handling Ecoflex was a bit more easy, also because the

mixture was less viscous, similar to spreading honey. Ultimately, all samples were cured at a constant room temperature of $23^{\circ}\text{C} \pm 0.5^{\circ}\text{C}$ and under environmental pressure conditions. The cured Mold Star could be removed from the molds after about an hour, while the samples made with Ecoflex were left to cure for about 24 hours.

5.1 Apparatus and Design

To measure the characteristics of these 8 different samples (Ecoflex and Mold Star in combination with the four different ferromagnetic powders), we utilized a planar sensing coil on a 2-layered printed circuit board.

To select an appropriate coil geometry and to ensure its reliability and repeatability, we measured the inductance of various coils using a Keysight E4990A impedance analyzer. The result can be found in Figure 7.

In this figure, we present various measurements of coils that were used in different applications discussed in this paper.

All self-wound coils were fabricated using a copper wire with a protective coating from Elektrisola (TW-A), with a diameter of 0.16 mm. Three variants were implemented: 20 turns with diameters of 15 mm and 20 mm, and 30 turns with a diameter of 15 mm. Additionally, coils from the Texas Instruments Reference Coil Board Evaluation Module¹ were utilized, including the PCB-J, featuring 30 turns, a diameter of 29 mm, a 0.15 mm trace width, and 2 layers; the PCB-K, featuring 35 turns, a diameter of 29 mm, an 0.2 mm trace width, and 4 layers; and the PCB-S, featuring 16 turns, a diameter of 10 mm, a 0.1 mm trace width, and 2 layers.

The measurements highlight key properties of various coils: (I) Soft magnetic cores consistently enhance the measured inductance, regardless of the coil geometry. (II) Wire-wound air coils exhibit a nearly constant inductance within the frequency range of 1 kHz to 1 MHz, making this range ideal for setting the measurement frequency in practical applications. The introduction of soft magnetic cores alters the inductance magnitude but does not affect its frequency dependency, indicating that the magnetization time of the ferromagnetic filler in the composite is shorter than $1\ \mu\text{s}$, leaving the measurement unaffected. (III) PCB coils generally have higher inductance, simplifying measurements. However, their elevated inductance, combined with parasitic capacitance, causes resonances near the reported frequency range, reducing the stability of measured inductance values. It is crucial to precisely fix the measurement frequency to isolate the effect of pressure.

The coil ultimately used in the following experiment is identified as PCB-J with a coreless inductance of $7.7\ \mu\text{H}$. The sensor capacitor was selected to be $68\ \mu\text{F}$. This coil was selected because it represents a good trade-off between practical size, high inductance, and absence of significant resonances in the relevant frequency range.

The coil on which the corresponding elastomer was placed was connected to TI's inductance measurement board (LDC1614). Whenever the magnetic elastomer was deformed (i.e. by applying a force), a change in the inductance of the sensing coil was measured and recorded. For evaluating the elastomer mixture we iteratively placed non-metallic weights on the respective samples, with weights going from 41 g to 357 g.

5.2 Results

Before we dive deeper into the quantitative data, we would like to briefly describe our subjective observations. It is immediately noticeable that the samples made with Mold Star appear somewhat firmer and more stable. The Ecoflex samples, on the other hand, have a slightly more gelatinous texture - though this does not mean they were less robust. They also had a slightly stickier surface. Nonetheless, it should be noted that all samples were of good quality. All samples were ferromagnetic, as confirmed by a simple magnet test in which we observed that a magnet adhered to the elastomer composites, cf. Figure 8(I).

Although all samples were ferromagnetic, a gradual color gradient was noticeable within them, cf. Figure 8. The material was slightly more transparent at the top, while the bottom tended to be grayer, suggesting a higher concentration of ferromagnetic particles there. This was particularly evident in samples where the particles were larger than $65\ \mu\text{m}$, cf. Figure 8 (E, G). The accumulation of more particles at the bottom can be explained by the particles being heavier and sinking during the curing process. This was especially noticeable in the samples made with Ecoflex, where the curing time was 24 hours. However, this had no significant impact on the measurement results. Overall, the gradient was significantly less noticeable in the samples containing very fine powder - see Figures 8 (F) and 8 (H) - as the powder had more difficulty sinking.

The normalized inductance change of the planar sensing coil, measured across 8 different samples under varying weights, is shown in Figure 9. The graphs display results for Mold Star (top) and Ecoflex (bottom) silicone cylinders, each embedded with one of the four filler materials: *Ancorsteel 1000C Powder* (A, E), *Iron Powder Fine* (B, F), *Iron Powder Coarse* (C, G), and *Magnetite Powder* (D, H). Each graph represents the average response and standard deviation of the sensors, based on three separate measurements.

All samples showed the expected response, with an increase in inductance as weight was applied, and illustrated in Figure 9. This response is due to two factors: First, the applied weight compresses the elastomer cylinders, expanding the diameter of the ferromagnetic cores near the planar coils. Second, compression increases the density of the ferromagnetic particles, thereby enhancing the material's effective permeability. The softer Ecoflex composites were tested with weights up to 217 g, as higher loads caused mechanical instability. Additionally, Ecoflex samples displayed significant saturation at weights above 100 g. However, Ecoflex offered higher sensitivity at lower weights, with approximately 0.3% change per 100 g, compared to 0.2% for Mold Star composites. All Ecoflex samples also exhibited noticeable hysteresis, attributed to the material's viscoelastic properties.

In contrast, the more rigid Mold Star composites could withstand higher pressure levels with much less saturation and significantly reduced hysteresis. Specifically, the combination of Mold Star and magnetite powder produced highly stable sensors, capable of reliably measuring weights above 300 g with virtually no hysteresis.

In summary, the harder Mold Star 31T samples showed lower sensitivity but provided more stable sensor readings, less hysteresis, and the ability to measure larger weights. On the other hand, the softer Ecoflex 00-30 samples were better suited for measuring lower

¹<https://www.ti.com/tool/LDCCOILEVM>

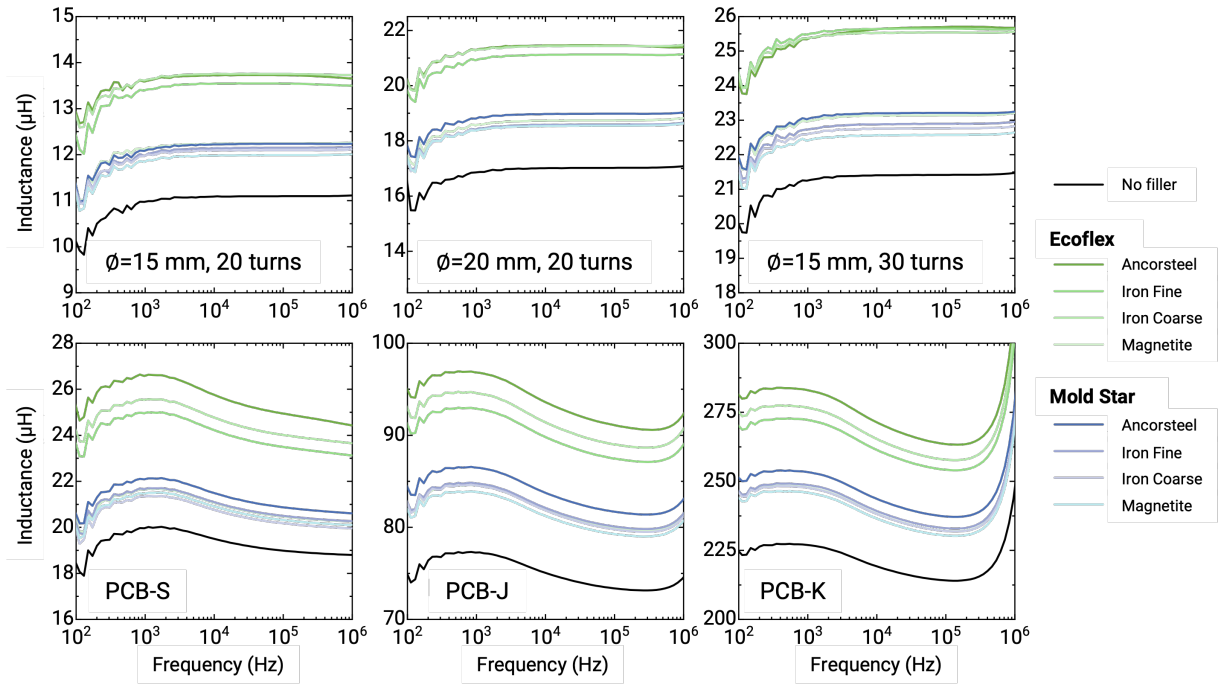


Figure 7: In our tests and applications, different coils were used. For the self-wound coils, three different geometries were utilized (top), while additionally prototyping coils on PCB boards were used (bottom).

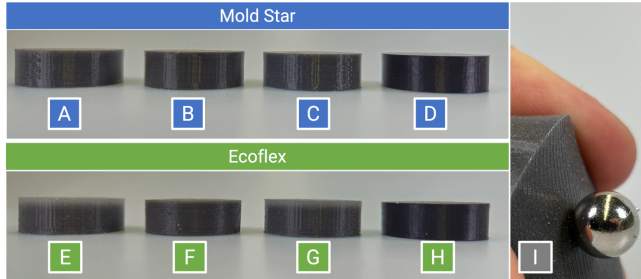


Figure 8: Using the softer Ecoflex in combination with ferromagnetic particles larger than 65 μm resulted in the particles settling to the bottom after a certain period of time. This effect was clearly visible in some samples (E, G). In contrast, this effect was not observed in other samples (F, H), where the powder was finer. Close-up images of the Mold Star samples (A-D) also showed that this phenomenon was absent, indicating that the particles were more evenly mixed with the elastomer. A magnet adhering to the silicone demonstrates the samples ferromagnetic properties (I).

pressures. According to these results, all samples are suitable for detecting minute relative pressure changes. The absolute inductance varies slightly when repeatedly removing and placing the same silicone sample on the coil. This is because of small differences in the manual positioning of the silicon. However, this is not an issue, as we are only interested in the relative inductance changes

when pressure is applied through weights. While Figure 9 shows that the inductance change relative to the pressure is not linear, the inductance and weight can be correlated and, according to the measurements, the Mold Star magnetite sample would be the most fitting, showing the lowest standard deviation for each weight level.

6 Design Exploration & Applications

To apply our sensors in real-world scenarios, we explored potential modifications, extensions, and use cases with an interdisciplinary focus group composed of professional UX designers, material designers, and material and computer scientists. The goal was not to create entirely new applications that could never be implemented with other sensing techniques but rather to demonstrate the versatility, and simplicity of the *SqueezeMe* concept. It was also important to show that different 3D geometries can achieve similarly good results, thus providing qualitative insights. Over a period of several weeks, we developed various prototypes and identified several benefits. In the following sections, we discuss our experiments and findings in detail.

6.1 Design Considerations

Resulting from our experiments we give a structured summary of design consideration which inform the design of a ferromagnetic silicone pressure sensor.

6.1.1 Size. Intuitively and also confirmed by the experiments of Ozioko et al. [24], we see that a smaller silicone sensor leads to smaller changes in inductance when compressed.

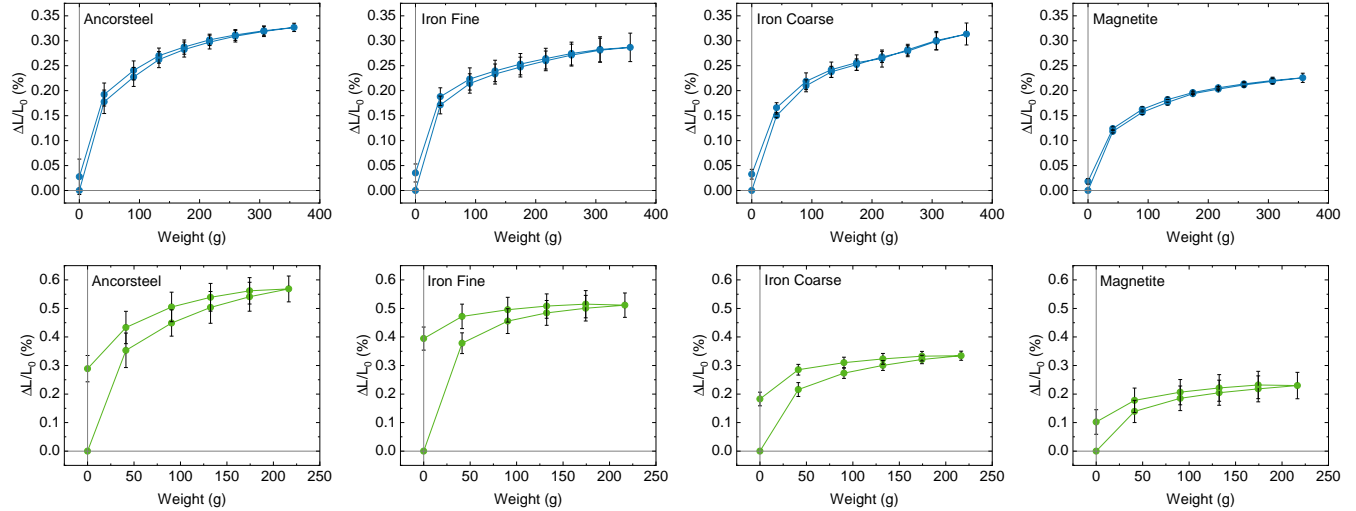


Figure 9: The graphs show the weight to inductance relation of 8 different silicone cylinders. The first row shows casts with Mold Star silicone while the lower show Ecoflex silicone. The different columns show the results of the filler materials (*Ancorsteel 1000C Powder*, *Iron Powder Fine*, *Iron Powder Coarse*, and *Magnetite Powder*). Every plot contains a hysteresis curve with each dot including error bars representing 3 individual measurements. The used sensor capacitor was 68 pF.

As mentioned in [3], the size of a sensor always has a significant impact on its application. It is important to use a coil that is appropriately sized for the corresponding silicone mold. Regardless of this, in the experiments we conducted with different sizes, all samples produced usable measurements. Therefore, the correct size should be determined more by the specific application. In the following applications, we will implement different sizes and shapes specifically for this purpose.

6.1.2 Silicone Geometry. The dimensions and geometry of the sensors are constrained by the coil size, the moldability of the silicone, and the sensitivity of the sensing electronics. To validate sensor functionality across diverse geometries, we explored various applications with different form factors, as outlined in Section 6.2.

6.1.3 Coil design. The coil can either be placed flat at the bottom or embedded directly into the mold. It is also possible to wrap an insulated wire, which allows for creating very thin and elongated silicone molds. All these implementation options enable us to cast highly complex shapes that also provide good measurement results. In all applications in which we embedded the coil directly into the cast silicone, we could get usable sensor data, e.g. sensing the compression of a squeezing controller. We also observed what Kawasetu et al. [16] describe that a coil size with smaller diameter yields a lower SNR for this type of sensor. Also, hand-wound coils, not created with perfect precision, proved to be well-suited for our applications.

6.1.4 Hardness. Choosing different levels of hardness also allows us to create either highly elastic applications or to build more rigid sensors. However, high elasticity does not necessarily mean a more stable sensor – the sensors provided similar results regardless of the hardness, but during testing, we found that softer Ecoflex resulted

in more sensitive sensors suitable for lower pressure values but with an increased hysteresis compared to Mold Star. When using softer silicones, it is definitely recommended to use very fine metal powder to prevent heavier metal particles from settling at the bottom during curing. This is particularly important with Ecoflex, as the curing process can take up to 24 hours.

6.1.5 Surface. We also observed that when casting very thin sheets of Ecoflex with heavier particles, the mixture often developed a slight stickiness. However, it is known that certain fillers can inhibit full curing of some elastomers. Components A and B were consistently mixed in a precise 50/50 ratio, as per the specifications. Even after about a week, the stickiness persisted. Nevertheless, this issue was less noticeable with thicker molds and did not occur when using iron powder. In contrast, all molds cast with Mold Star, even with larger iron particles, had a more "natural" feel.

6.2 Applications

In this section and the supplementary video, we present various application scenarios that demonstrate the benefits of our sensors. All the examples were created using both Ecoflex and Mold Star silicone casts. For all demonstration applications, we utilized the inductance-to-digital converter (LDC) from Texas Instruments (LDC1614).

The processed data were then either visualized on an OLED display based on the ESP32 controller and/or sent to a custom application on a Windows PC via the OSC protocol. For the demo applications on the PC we used C# in combination with Unity. The software used for reading out the sensor values used in the demonstrations is provided in the supplementary material.

6.2.1 Sensitive and light-weight measurement. The experiments revealed that the elastomer, especially when combined with magnetized powder, is exceptionally well-suited for measuring very light weights, and it also has a very high dynamic range. In comparison to resistive measurements it showed very low drift. The more flexible the silicone, the better the results when measuring light forces, while harder elastomers are better to measure heavier objects.

For instance, very light materials can be measured, as shown in Figure 10. In these examples, we used a silicone mold with a diameter of 2 cm and a thickness of 1 cm. The base material was Ecoflex 00-50 or Mold Star T31, combined with Magnetite Powder, as Experiment 2 demonstrated reliable measurements with this combination. Here, we developed a weight sensor for lightweight objects. Figure 10 (A) displays a cotton ball (weight: 2.75 g) on the sensors and the corresponding inductance measurements when the cotton ball was placed on and removed from both Ecoflex and Mold Star sensors. The results show that the placement of the cotton ball on the sensor results in a significant increase in inductance around 10 s, compared to the baseline when the cotton ball was absent. As expected from such a low weight, there was no visible hysteresis. Additionally, the softer Ecoflex proved slightly more sensitive, with a larger inductance change compared to the Mold Star sensor. The data also show not only the static weight but also peaks when the cotton ball was placed and removed from the sensor (around 7 s and 14 s). These peaks reflect the additional forces applied during the interaction, highlighting the sensor's fast response time and ability to detect a very soft human touch.

To further demonstrate the sensor's high dynamic range, Figures 10 (B) and 10 (C) show the measurement of a figurine made from NanoBlock bricks (with individual brick dimensions of 4 mm × 4 mm × 3 mm, weighing 0.04 g each). In this example, the sensor measures the figurine both with and without a few missing bricks. Despite the relatively heavy weight of the figurine biasing the sensor, it was still able to detect the subtle change in weight caused by the missing bricks.

In the final demonstration, the sensor's response to a large number of small plastic particles being poured onto it is shown in Figure 10 (D). Two effects are visible: first, during the pouring phase, the impact of individual particles caused multiple peaks in the sensor signal. Second, after the pouring stopped at around 12 s, the sensor signal quickly stabilized, reflecting the cumulative weight of all the particles.

The advantage of our approach over a conventional postal scales utilizing a deformed spring and/or load cell is that in our implementation, the sensing material itself is highly flexible and can therefore be integrated into various other applications, where a high deformation of the tool is required. This flexibility allows the material to be cast into a shape (e.g., into a tool of a robot arm) while still enabling force measurement with high precision. The key to this implementation is effective shielding, ensuring that the sensor is not negatively affected by external interference.

6.2.2 4-Way Controller. In the next application, we wanted to explore whether more complex silicone molds are feasible and how to determine the ideal combination with the coils. Our mold consisted of a suction cup at the bottom and a knob on the surface, which is intended to be operated by the user, similar to a joystick. Gentle

tilting motions in either direction cause pressure changes, which can be used to determine the four directions as well as a push down action.

Overall, we implemented different versions of this application - also to see the corresponding pros and cons. In all versions, the silicone mold was created using Mold Star with Shore A-30 and Ancorsteel 1000C Powder (with a mixture as described in the apparatus of the experiment).

In the first version (A), we cast the mold in a single pour, meaning the entire controller was essentially made from ferromagnetic silicone. We then placed one, two, and four coils on the underside to detect movements. The slightest changes could be easily detected and were projected onto two axes (forward, backward, left, and right). Although two coils would have been sufficient, we would recommend to choose four to achieve a better accuracy. During testing, we noticed that the proximity of a finger significantly influenced the measurement, which could be seen as both an advantage and a disadvantage. To counteract this effect, we created a second mold (B) where the upper part, where the finger touches, was made from non-ferromagnetic silicone. Similarly, we developed a third adapted version (C), where we replaced the joystick itself with a non-conductive material to ensure that contact with fingers did not cause any interference. Both of these versions provided better measurement results than version (A). Finally, we created two additional molds where we embedded the coil directly into the joystick form (D, E). In the first of these (D), we embedded a single wire wound coil (Elektrisola, TW-A, 0.16 mm) with 30 turns and a diameter of 20 mm, while in the second version (E), we embedded two coils with the same specifications.

The negative molds for casting were created using a 3D printer. Given the complexity of a detailed 3D silicone mold, it is recommended to design the negative mold in multiple parts that can be disassembled after pouring the silicone, as the silicone adheres to the mold very well. For this application, we used Mold Star T31 silicone combined with AncorSteel 1000C Powder, as we had very positive experiences with Mold Star, particularly due to its ease of handling and quicker curing time. All samples were ready in about an hour and could be integrated with the hardware for combined use, cf. Figure 11 (E-F).

6.2.3 Wristband for measuring arterial pulsations. Inspired by Kumar et al. [19], we developed a smart silicone wristband capable of measuring arterial pulsations. Instead of designing a complete smart silicone band, the sensor was placed beneath the existing wristband of a Lilygo T-Watch S3 (which is based on a ESP32 architecture).

To achieve optimal measurement results, we designed a custom 3D-printed mold that allowed us to create a silicone structure comprising of a silicone cylinder with a circular trench on one side. A coil was placed inside this trench. We aimed to test different elastomer hardness levels, so we prepared samples with both Ecoflex Shore 00-30 and 00-50 - achieving an ultra-soft solution. Both variants were mixed with the very fine Magnetite Powder and then cast into the 3D mold. Finally, the cast discs were placed on the inside of the wrist to ensure optimal pulse measurement, with a band gently applying pressure to keep the sensor in place during the measurement, as shown in Figure 12.

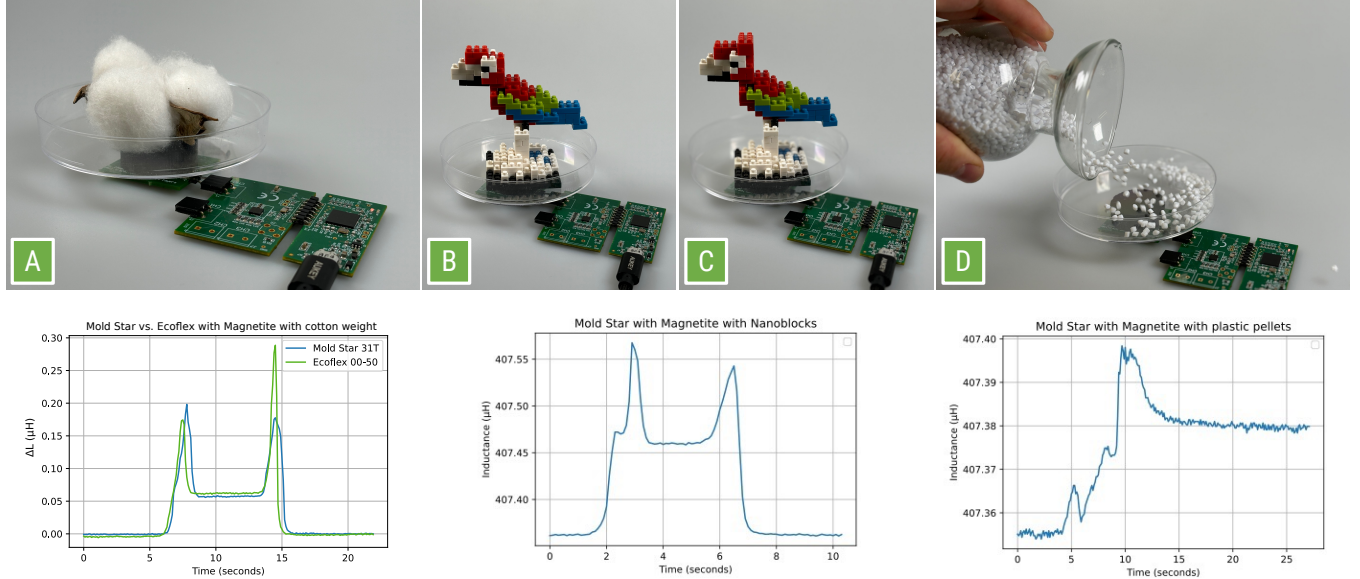


Figure 10: We implemented a weighting application in we which measured the influence of different weights on the inductance. We used a Mold Star cylinder with Magnetite Powder and placed a cotton ball (A), a macaw figure from Nanoblocks (B, C), and individual plastic pellets (D) onto a petri dish.

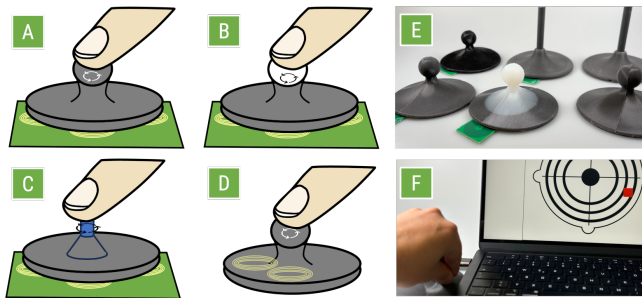


Figure 11: Different approaches were explored in developing a 4-way controller to determine the most effective method. On one hand, various silicone molds were used in combination with coils mounted on the underside (A-C), and on the other hand, two versions with embedded coils were implemented (D). Several prototypes were created (E). Some were combined with coils placed underneath the controller, while others had custom-wound coils embedded directly into the elastomer. Both versions produced reliable results and were integrated with specific apps (e.g., Crosshair App) (F).

The coil was reconnected to the LDC1614 and paired with a 1000 pF capacitor. For the measurement, the sensor was positioned on the participant's right wrist, directly over the radial artery, with participants instructed to sit in a relaxed position. The sensor then measured the physical pulsatile changes in the radial artery, providing an alternative to conventional ultrasound methods and replacing resistive-based sensors often lacking adequate sensitivity and linearity. The raw sensor signal was filtered using a second-order IIR Chebyshev band-pass filter to eliminate offsets caused by



Figure 12: The mold used for the wristband was designed in such a way (A) that it allowed us to easily place the coil directly into the mold (B). Combined with a wrist strap, this setup enabled us to accurately measure the pulse (C).

varying initial contact pressures and low frequency measurement artifacts.

This example demonstrates that even the slightest pressure changes can be detected. Following Kumar's implementation [19], the system's signal-to-noise ratio, free from motion artifacts, offers a route towards analyzing pulsation components such as blood pressure, cardiac output, vascular assessment, arterial diseases, arterial compliance, aging, venous assessment, and breathing rate. Compared to optical pulse measurement systems (PPM), this approach offers the advantage of measuring additional parameters, including arterial stiffness and vascular conditions [19]. However, due to muscle movements generating noise, the sensor should be relatively small and positioned to primarily detect the pulsatile expansion of wrist blood vessels for optimal pulse rate measurement.

6.2.4 Squeezing controller. Finally, inspired by Aigner et al. [2] as an experimental user interface, we developed a squeeze controller (see Figure 13) utilizing an embedded coil inside a silicone handle. To explore this input modality, we also created a simple vertex shader in Unity to deform 3D meshes.

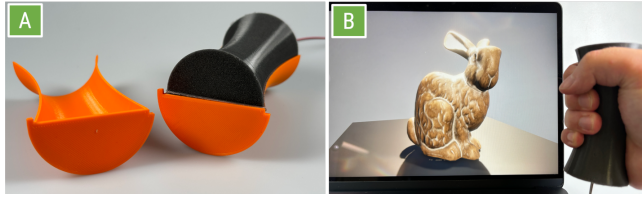


Figure 13: In a Unity-based 3D application, users can manipulate the Stanford Bunny using our Squeezing Controller (A). They have the option to either gently hold the controller or apply force to compress the 3D bunny model (B). This effect is achieved through a Vertex Shader implementation.

The embedded coil used in this example was a PCB coil, with a diameter of 5 mm, 20 turns, a trace width of 0.10 mm, a trace spacing of 0.10 mm, 4 layers, and a capacitor with 330 pF. In this example, the coil was carefully placed into the mold during the silicone casting process before the remaining part of the mold was filled with the material. This application example demonstrates that a coil can be embedded even in more complex shapes, allowing for creating soft tangible user interfaces. This demonstrator could serve as a representative model for a sensor that could be attached to a robotic tool to detect even small forces, such as during a collision, or for highly flexible silicone-based robots where force measurement is required.

6.2.5 Air pressure measurement. In the application shown in Figure 14, we aimed to test whether air pressure could be measured. In the first experiment, depicted in Figure 14 (A), we used a sample from our previous experiment (Mold Star with Magnetite powder) and placed it, along with an induction coil (26 turns, etc.), in a vacuum chamber. The air was gradually removed until the pressure was approximately 0.8 bar below atmospheric pressure, resulting in an absolute pressure of about 0.2 bar inside the chamber. This state was maintained for around 10 seconds before the air was reintroduced, allowing the pressure to return to normal. The sensor successfully captured the entire sequence of events, as shown in Figure 14 (A). The decrease in air pressure caused an increase in inductance because the elastomer expanded, effectively enlarging the ferromagnetic core of the sensing coil.

Next, we utilized the sensor to monitor the expansion of the rubber tire of a bike while the air pressure inside the tire increased. The pressure between the tire and tube served as a proxy for detecting the air pressure inside the tube. Unlike in the previous example, the inductance increase here is linked to the ferromagnetic particles coming closer to the coil by compression of the silicone. Here a suitable sensor is placed between the tire and the inner tube of a bicycle. Figure 14 (B) illustrates the placement of the sensor. After placing the sensor inside the tire, we could determine whether the tire pressure was high (i.e., the tire was inflated) or whether the air had been released. To test its durability, we installed the sensor on a bike used daily. After three months of rides, the sensor remained functional, as shown in the graph in Figure 14 (C).

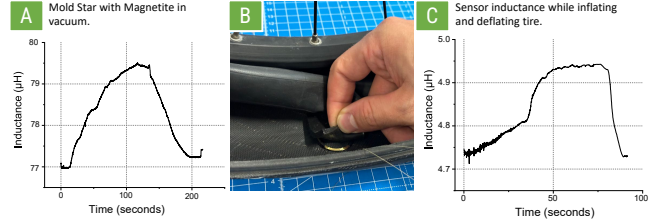


Figure 14: The chart shows the inductance change when a sensor (Mold Star with magnetite) is exposed to a vacuum (A). The graph shows the pressure decreasing while the inductance is increasing. After 100 s the vacuum chamber is again filled with air, equalizing the inside and outside air pressure. In another application, a sensor we designed, was placed between the tube and the rim of a bicycle (B), and then the tire was inflated and deflated, which can be seen in the corresponding graph (C).

7 Discussion & Limitations

The findings from our evaluation, as well as the design and implementation of the different applications, present a clear picture: Both Ecoflex and Mold Star can be effectively combined with ferromagnetic particles, including *Ancorsteel 1000C Powder*, *Iron Powder Fine*, *Iron Powder Coarse*, and *Magnetite Powder*. When selecting ferromagnetic particles, it has been found that choosing very fine-grained (powder-like) particles (30 µm) can be advantageous, because these allow for a somewhat more homogeneous silicone mold as the particles do not settle at the bottom. In most applications, Mold Star was used as it only required about an hour to cure. When selecting the coil, we tested three possible setups:

- a coil placed underneath the silicone mold,
- a coil embedded within the silicone mold, and
- a coil wrapped around the silicone mold.

Depending on the application, one of these three setups may be more advantageous. All three configurations provide reliable data from a measurement perspective and we were particularly pleased with the results of the embedded coil designs as they were handmade.

It is worth noting that even the handmade coils delivered relatively good results. It turned out that the insulated copper wires from Elektrisola (TW-A), with a thickness of 0.16 mm, were very well suited for this purpose. We typically wound coils with about 30 turns. Here, it was also evident that more turns led to higher inductivity, but it was not crucial for the wire to be wound with 100% precision.

According to the Texas Instruments datasheet, and our experience it is crucial to ensure that the magnetic field around the sensing coil is not affected by factors other than the deformation of the ferromagnetic elastomer. Movements of nearby ferromagnetic objects, permanent magnets, or strong electric currents can interfere with measurements. Additionally, conductive objects that capacitively couple with the readout can disrupt the results. It is recommended to keep potential interfering objects at a sufficient distance from the sensor to avoid such effects. If a nearby conductor cannot be moved farther away, reducing the sensor size should be

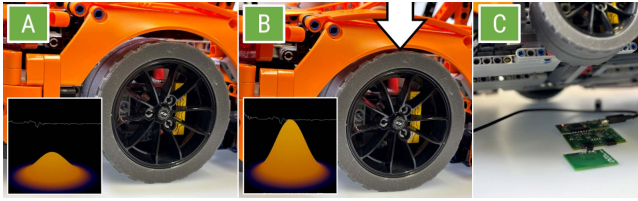


Figure 15: By using Ecoflex with a Shore A 50 hardness for the tires, combined with an inductive coil, we can measure the tire pressure while the car is in motion.

considered. Although this might lower the measurement resolution, it can minimize parasitic coupling, especially if the distance exceeds the coil's radius. Lastly, interference can be mitigated by using appropriate shielding, such as a static grounded conductor made from magnetic shielding material, like ferrite, which can protect against both magnetic and electric field interference.

After implementing the various applications, we aimed to further evaluate silicone molds with a Shore A hardness of 50 to determine if harder molds could also provide measurable results, potentially combining the high sensitivity of Ecoflex with the stability of Mold Star. Figure 15 shows a sample created using Ecoflex 00-50. We replicated the rubber tires of a LEGO Technic vehicle using Ecoflex mixed with AncorSteel 1000C Powder and cast them into a suitable negative mold. The result was a rubber tire mounted on the vehicle. In combination with an induction coil attached to the chassis, we were able to measure pressure changes while driving.

A potential extension would be to produce very thin rubber bands, which could then be wrapped with copper wire so that the coil encircles the "thread". Finally, an appropriate thread could be created using a braiding machine to create a sensor yarn.

8 Conclusion and Future Work

In this paper, we presented SqueezeMe, a soft and highly stretchable inductive sensor based on ferromagnetic elastomers, demonstrating its potential for various applications. The sensor's design, combining silicone elastomers with ferromagnetic fillers, enabled precise detection of very small pressure changes. Through a series of experiments, we evaluated different material combinations and fabrication techniques, identifying optimal configurations that balance sensitivity and mechanical robustness. The implementation of the sensor in applications such as sensitive weight measurement and pulse monitoring highlighted its versatility and adaptability in real-world scenarios.

For future work, we would like to focus on enhancing the sensor's sensitivity, durability, and sustainability by exploring new elastomer formulations and filler materials with higher magnetic permeability. Additionally, we plan to investigate advanced manufacturing techniques, such as 3D printing and multi-material molding, to further refine sensor geometries and improve performance consistency. Furthermore, we aim to develop a stretchable rubber band that would be woven with threads and integrated as a sensor into a textile. Expanding the range of applications, including integration into complex soft robotic systems, will also be key areas of exploration.

By addressing these challenges, we aim to extend the capabilities of SqueezeMe and contribute to the advancement of flexible, stretchable sensors for next-generation human-machine interfaces and biomedical devices.

Acknowledgments

This work was supported by the Autonomous Province of Bozen-Bolzano-South Tyrol's European Regional Developmental Fund (ERDF) Program under Project EFRE/FESR 1011- SmartCover.

References

- [1] Faheem Ahmed, Afaque Manzoor Soomro, Hina Ashraf, Abdul Rahim, Arun Asif, Bushra Jawed, Muhammad Waqas, and Kyung Hyun Choi. 2022. Robust ultrasensitive stretchable sensor for wearable and high-end robotics applications. *Journal of Materials Science: Materials in Electronics* 33, 35 (Dec. 2022), 26447–26463. doi:10.1007/s10854-022-09324-0
- [2] Roland Aigner, Mira Alida Haberfellner, and Michael Haller. 2022. spaceR: Knitting Ready-Made, Tactile, and Highly Responsive Spacer-Fabric Force Sensors for Continuous Input. In *Proceedings of the 35th Annual ACM Symposium on User Interface Software and Technology*. ACM, Bend OR USA, 1–15. doi:10.1145/3526113.3545694
- [3] Jason Alexander, John Hardy, and Stephen Wattam. 2014. Characterising the Physicality of Everyday Buttons. In *Proceedings of the Ninth ACM International Conference on Interactive Tabletops and Surfaces*. ACM, Dresden Germany, 205–208. doi:10.1145/2669485.2669519
- [4] Tristan Beven, Thuong Hoang, Marcus Carter, and Bernd Ploderer. 2016. HandLog: a deformable tangible device for continuous input through finger flexion. In *Proceedings of the 28th Australian Conference on Computer-Human Interaction (OzCHI '16)*. Association for Computing Machinery, New York, NY, USA, 595–604. doi:10.1145/3010915.3010933
- [5] Nicholas Biria, Pallavi Dhangat, and Joseph R. Davidson. 2020. A Review of Magnetic Elastomers and Their Role in Soft Robotics. *Frontiers in Robotics and AI* 7 (Oct. 2020). doi:10.3389/frobt.2020.588391 Publisher: Frontiers.
- [6] Alberto Boem and Giovanni Maria Troiano. 2019. Non-Rigid HCI: A Review of Deformable Interfaces and Input. In *Proceedings of the 2019 on Designing Interactive Systems Conference*. ACM, San Diego CA USA, 885–906. doi:10.1145/3322276.3322347
- [7] Armandka Byberi, Maryam Ravan, and Reza K. Amineh. 2023. GloveSense: A Hand Gesture Recognition System Based on Inductive Sensing. *IEEE Sensors Journal* 23, 9 (May 2023), 9210–9219. doi:10.1109/JSEN.2023.3262359
- [8] Julio C. Costa, Filippo Spina, Pasindu Lugoda, Leonardo Garcia-Garcia, Daniel Roggen, and Niko Münzenrieder. 2019. Flexible Sensors—From Materials to Applications. *Technologies* 7, 2 (June 2019), 35. doi:10.3390/technologies7020035 Number: 2 Publisher: Multidisciplinary Digital Publishing Institute.
- [9] Sean Follmer, Daniel Leithinger, Alex Olwal, Nadia Cheng, and Hiroshi Ishii. 2012. Jamming user interfaces: programmable particle stiffness and sensing for malleable and shape-changing devices. In *Proceedings of the 25th annual ACM symposium on User interface software and technology (UIST '12)*. Association for Computing Machinery, New York, NY, USA, 519–528. doi:10.1145/2380116.2380181
- [10] Sean Follmer, Daniel Leithinger, Alex Olwal, Akimitsu Hogge, and Hiroshi Ishii. 2013. inFORM: dynamic physical affordances and constraints through shape and object actuation. In *Proceedings of the 26th annual ACM symposium on User interface software and technology*. ACM, St. Andrews Scotland, United Kingdom, 417–426. doi:10.1145/2501988.2502032
- [11] Jun Gong, Olivia Seow, Cedric Honnet, Jack Forman, and Stefanie Mueller. 2021. MetaSense: Integrating Sensing Capabilities into Mechanical Metamaterial. In *The 34th Annual ACM Symposium on User Interface Software and Technology*. ACM, Virtual Event USA, 1063–1073. doi:10.1145/3472749.3474806
- [12] Jun Gong, Yu Wu, Lei Yan, Teddy Seyed, and Xing-Dong Yang. 2019. Tessutivo: Contextual Interactions on Interactive Fabrics with Inductive Sensing. In *Proceedings of the 32nd Annual ACM Symposium on User Interface Software and Technology*. ACM, New Orleans LA USA, 29–41. doi:10.1145/3332165.3347897
- [13] Jun Gong, Xin Yang, Teddy Seyed, Josh Urban Davis, and Xing-Dong Yang. 2018. Indutivo: Contact-Based, Object-Driven Interactions with Inductive Sensing. In *Proceedings of the 31st Annual ACM Symposium on User Interface Software and Technology*. ACM, Berlin Germany, 321–333. doi:10.1145/3242587.3242662
- [14] Liang He, Gierad Laput, Eric Brockmeyer, and Jon E. Froehlich. 2017. SqueezePulse: Adding Interactive Input to Fabricated Objects Using Corrugated Tubes and Air Pulses. In *Proceedings of the Eleventh International Conference on Tangible, Embedded, and Embodied Interaction (TEI '17)*. Association for Computing Machinery, New York, NY, USA, 341–350. doi:10.1145/3024969.3024976

- [15] Faiza Jabbar, Afaque Soomro, Jae-Wook Lee, Muhsin Ali, Young Kim, Sang-Ho Lee, and Kyung Choi. 2020. Robust Fluidic Biocompatible Strain Sensor Based on PEDOT:PSS/CNT Composite for Human-wearable and High-end Robotic Applications. *Sensors and Materials* 32 (Nov. 2020), 1. doi:10.18494/SAM.2020.3085
- [16] Takumi Kawasetsu, Takato Horii, Hisashi Ishihara, and Minoru Asada. 2018. Flexible Tri-Axis Tactile Sensor Using Spiral Inductor and Magnetorheological Elastomer. *IEEE Sensors Journal* 18, 14 (July 2018), 5834–5841. doi:10.1109/JSEN.2018.2844194 Conference Name: IEEE Sensors Journal.
- [17] Gerald Kettlgruber, Doris Danninger, Richard Moser, Michael Drack, Christian M. Siket, Daniela Wirthl, Florian Hartmann, Guoyong Mao, Martin Kaltenbrunner, and Siegfried Bauer. 2020. Stretch-Safe: Magnetic Connectors for Modular Stretchable Electronics. *Advanced Intelligent Systems* 2, 8 (2020), 2000065. doi:10.1002/aisy.202000065 _eprint: <https://onlinelibrary.wiley.com/doi/pdf/10.1002/isy.202000065>
- [18] Dimitri Kokkinis, Manuel Schaffner, and André R. Studart. 2015. Multimaterial magnetically assisted 3D printing of composite materials. *Nature Communications* 6, 1 (Oct. 2015), 8643. doi:10.1038/ncomms9643 Publisher: Nature Publishing Group.
- [19] Nimal Jagadeesh Kumar, Alexander Johnson, Robert Cobden, George Valsamakis, J.Gene Gristock, Arash Pouryazdan, Daniel Roggen, and Niko Münzenrieder. 2023. A Flexible Inductive Sensor for Non-Invasive Arterial Pulse Measurement. In *2023 IEEE SENSORS*. IEEE, Vienna, Austria, 1–4. doi:10.1109/SENSORS56945.2023.10324884
- [20] Jian Mao, Zidong He, Yuanzhao Wu, Jinwei Cao, Shijing Zhao, Bin Chen, Jie Shang, Yiwei Liu, and Run-Wei Li. 2024. Ultra-high resolution, multi-scenario, super-elastic inductive strain sensors based on liquid metal for the wireless monitoring of human movement. *Materials Advances* 5 (June 2024). doi:10.1039/D4MA00140K
- [21] Vinh Nguyen, Pramod Kumar, Sang Ho Yoon, Ansh Verma, and Karthik Ramani. 2015. SOFTii: Soft Tangible Interface for Continuous Control of Virtual Objects with Pressure-based Input. In *Proceedings of the Ninth International Conference on Tangible, Embedded, and Embodied Interaction (TEI '15)*. Association for Computing Machinery, New York, NY, USA, 539–544. doi:10.1145/2671199.2687898
- [22] Simon Olberding, Sergio Soto Ortega, Klaus Hildebrandt, and Jürgen Steimle. 2015. Foldio: Digital Fabrication of Interactive and Shape-Changing Objects With Foldable Printed Electronics. In *Proceedings of the 28th Annual ACM Symposium on User Interface Software & Technology*. ACM, Charlotte NC USA, 223–232. doi:10.1145/2807442.2807494
- [23] Oliver Ozioko, Marion Hersh, and Ravinder Dahiya. 2019. Inductance-Based Soft and Flexible Pressure Sensors using Various Compositions of Iron Particles. In *2019 IEEE SENSORS*. IEEE, Montreal, QC, Canada, 1–4. doi:10.1109/SENSORS43011.2019.8956646
- [24] Oliver Ozioko, Marion Hersh, and Ravinder Dahiya. 2019. Inductance-Based Soft and Flexible Pressure Sensors using Various Compositions of Iron Particles. In *2019 IEEE SENSORS*. IEEE, Montreal, QC, Canada, 1–4. doi:10.1109/SENSORS43011.2019.8956646
- [25] Gayoung Park, Hyun-Joong Chung, Kwanghee Kim, Seon Ah Lim, Jiyoung Kim, Yun-Soung Kim, Yuhao Liu, Woon-Hong Yeo, Rak-Hwan Kim, Stanley S. Kim, Jong-Seon Kim, Yei Hwan Jung, Tae-Il Kim, Cassian Yee, John A. Rogers, and Kyung-Mi Lee. 2014. Immunologic and tissue biocompatibility of flexible/stretchable electronics and optoelectronics. *Advanced Healthcare Materials* 3, 4 (April 2014), 515–525. doi:10.1002/adhm.201300220
- [26] Patrick Parzer, Florian Perteneder, Kathrin Probst, Christian Rendl, Joanne Leong, Sarah Schuetz, Anita Vogl, Reinhard Schwedauer, Martin Kaltenbrunner, Siegfried Bauer, and Michael Haller. 2018. RESi: A Highly Flexible, Pressure-Sensitive, Imperceptible Textile Interface Based on Resistive Yarns. In *Proceedings of the 31st Annual ACM Symposium on User Interface Software and Technology (UIST '18)*. Association for Computing Machinery, New York, NY, USA, 745–756. doi:10.1145/3242587.3242664
- [27] Martin Schmitz, Jürgen Steimle, Jochen Huber, Niloofar Dezfuli, and Max Mühlhäuser. 2017. Flexibles: Deformation-Aware 3D-Printed Tangibles for Capacitive Touchscreens. In *Proceedings of the 2017 CHI Conference on Human Factors in Computing Systems (CHI '17)*. Association for Computing Machinery, New York, NY, USA, 1001–1014. doi:10.1145/3025453.3025663
- [28] Carsten Schwegel, Ivan Poupyrev, and Eiji Mori. 2004. Gummi: a bendable computer. In *Proceedings of the SIGCHI Conference on Human Factors in Computing Systems (CHI '04)*. Association for Computing Machinery, New York, NY, USA, 263–270. doi:10.1145/985692.985726
- [29] Erh-li Early Shen, Sung-sheng Daniel Tsai, Hao-hua Chu, Yung-jen Jane Hsu, and Chi-wen Euro Chen. 2009. Double-side multi-touch input for mobile devices. In *CHI '09 Extended Abstracts on Human Factors in Computing Systems (CHI EA '09)*. Association for Computing Machinery, New York, NY, USA, 4339–4344. doi:10.1145/1520340.1520663
- [30] Cameron Steer, Kim Sauvé, Anika Jain, Omosunmisola Lawal, Michael J Proulx, Crescent Jicoli, and Jason Alexander. 2024. Squishy, Yet Satisfying: Exploring Deformable Shapes' Cross-Modal Correspondences with Colours and Emotions. In *Proceedings of the CHI Conference on Human Factors in Computing Systems*. ACM, Honolulu HI USA, 1–20. doi:10.1145/3613904.3641952
- [31] Jing Sun, Shaobing Zhou, Peng Hou, Yuan Yang, Jie Weng, Xiaohong Li, and Mingyuan Li. 2007. Synthesis and characterization of biocompatible Fe_3O_4 nanoparticles. *Journal of Biomedical Materials Research Part A* 80A, 2 (Feb. 2007), 333–341. doi:10.1002/jbm.a.30909
- [32] Marc Teyssier, Gilles Bailly, Catherine Pelachaud, Eric Lecolinet, Andrew Conn, and Anne Roudaud. 2019. Skin-On Interfaces: A Bio-Driven Approach for Artificial Skin Design to Cover Interactive Devices. In *Proceedings of the 32nd Annual ACM Symposium on User Interface Software and Technology*. ACM, New Orleans LA USA, 307–322. doi:10.1145/3332165.3347943
- [33] C. Thébault, M. Marmiesse, C. Naud, K. Pernet-Gallay, E. Billiet, H. Joisten, B. Diény, M. Carrière, Y. Hou, and R. Morel. 2021. Magneto-mechanical treatment of human glioblastoma cells with engineered iron oxide powder microparticles for triggering apoptosis. *Nanoscale Advances* 3, 21 (2021), 6213–6222. doi:10.1039/D1NA00461A
- [34] Muhammad Waqas, Afaque Manzoor Soomro, Shamshad Ali, Suresh Kumar, Sattar Chan, Kashif Hussain, Fida Hussain Memon, and Shoib Ahmed Shaikh. 2020. Multifunctional Cathodic Interlayer with Polysulfide Immobilization Mechanism for High-Performance Li-S Batteries. *ChemistrySelect* 5, 38 (2020), 12009–12019. doi:10.1002/slct.202003381 _eprint: <https://onlinelibrary.wiley.com/doi/pdf/10.1002/slct.202003381>
- [35] Martin Weigel, Tong Lu, Gilles Bailly, Antti Oulasvirta, Carmel Majidi, and Jürgen Steimle. 2015. iSkin: Flexible, Stretchable and Visually Customizable On-Body Touch Sensors for Mobile Computing. In *Proceedings of the 33rd Annual ACM Conference on Human Factors in Computing Systems (CHI '15)*. Association for Computing Machinery, New York, NY, USA, 2991–3000. doi:10.1145/2702123.2702391
- [36] Michael Wessely, Theophanis Tsandilas, and Wendy E. Mackay. 2016. Stretchis: Fabricating Highly Stretchable User Interfaces. In *Proceedings of the 29th Annual Symposium on User Interface Software and Technology (UIST '16)*. Association for Computing Machinery, New York, NY, USA, 697–704. doi:10.1145/2984511.2984521